

Semileptonic weak decays of anti-triplet charmed baryons in the light-front formalism

C.Q. Geng^{1,2,3}, Chia-Wei Liu^{1,2,3} and Tien-Hsueh Tsai³

¹*School of Fundamental Physics and Mathematical Sciences,*

Hangzhou Institute for Advanced Study, UCAS, Hangzhou 310024, China

²*International Centre for Theoretical Physics Asia-Pacific, Beijing/Hangzhou, China*

³*Department of Physics, National Tsing Hua University, Hsinchu 300, Taiwan*

(Dated: March 5, 2021)

Abstract

We systematically study the semileptonic decays of $\mathbf{B}_c \rightarrow \mathbf{B}_n \ell^+ \nu_\ell$ in the light-front constituent quark model, where \mathbf{B}_c represent the anti-triplet charmed baryons of $(\Xi_c^0, \Xi_c^+, \Lambda_c^+)$ and \mathbf{B}_n correspond to the octet ones. We determine the spin-flavor structures of the constituents in the baryons with the Fermi statistics and calculate the decay branching ratios (\mathcal{B} s) and averaged asymmetry parameters (α s) with the helicity formalism. In particular, we find that $\mathcal{B}(\Lambda_c^+ \rightarrow \Lambda e^+ \nu_e, n e^+ \nu_e) = (3.55 \pm 1.04, 0.36 \pm 0.15)\%$, $\mathcal{B}(\Xi_c^+ \rightarrow \Xi^0 e^+ \nu_e, \Sigma^0 e^+ \nu_e, \Lambda e^+ \nu_e) = (11.3 \pm 3.35), 0.33 \pm 0.09, 0.12 \pm 0.04\%$ and $\mathcal{B}(\Xi_c^0 \rightarrow \Xi^- e^+ \nu_e, \Sigma^- e^+ \nu_e) = (3.49 \pm 0.95, 0.22 \pm 0.06)\%$. Our results agree with the current experimental data. Our prediction for $\mathcal{B}(\Lambda_c^+ \rightarrow n e^+ \nu_e)$ is consistent with those in the literature, which can be measured by the charm-facilities, such as BESIII and BELLE. Some of our results for the $\Xi_c^{+(0)}$ semileptonic channels can be tested by the experiments at BELLE as well as the ongoing ones at LHCb and BELLEII.

I. INTRODUCTION

In the recent few years, there have been two important experiments in charmed baryon physics. One is the measurement of the absolute branching ratios of $\mathcal{B}(\Xi_c^0 \rightarrow \Xi^- \pi^+) = (1.8 \pm 0.5)\%$ [1] and $\mathcal{B}(\Xi_c^+ \rightarrow \Xi^- \pi^+ \pi^+) = (2.86 \pm 1.21 \pm 0.38)\%$ [2] from the Belle Collaboration, and the other is the most precise measurement of the Ξ_c^0 's lifetime of $\tau_{\Xi_c^0} = 154.5 \pm 1.7 \pm 1.6 \pm 1.0$ fs from the LHCb Collaboration [3], which significantly deviates from the past world averaged value of $\tau_{\Xi_c^0} = 112_{-10}^{+13}$ fs in PDG [4]. Both of them bring us new hints as well as new problems in charm physics. We are now in a precision-era of charm physics. It is expected that as more high quality data will be accumulated in the future, stronger constraints on various baryonic QCD models as well as physics beyond the standard model can be given.

Recently, the anti-triplet charm baryon decays have been extensively discussed in the literature. However, due to the large non-perturbative effects from the quantum chromodynamics (QCD), the decay amplitudes and observables of hadrons are very hard to obtain from the QCD first principle. To avoid the difficulties, various charmed baryon decay processes have been studied based on the flavor symmetry of $SU(3)_f$, such as semi-leptonic, two-body and three-body non-leptonic decays, to get reliable results [5–24]. It is known that $SU(3)_f$ is an approximate symmetry, resulting in about 10% of uncertainties for the predictions inherently. Moreover, the $SU(3)_f$ symmetry itself does not directly reveal any clue about the QCD dynamics. In fact, its applications heavily rely on the experimental data as inputs. In order to have precise calculations, we need a specific dynamical QCD model to understand each decay process. For simplicity, we only discuss the semi-leptonic processes of the anti-triplet charmed baryons in this study, which involve purely factorizable contributions. There are several theoretical calculations on these decay processes with different QCD frameworks in the literature [25–34].

The light front (LF) QCD formalism in the quark model is a consistent relativistic approach, which has been tested successfully in the mesonic and light quark sectors in early times [35, 36]. Because of these successes, it has been used in other generalized systems, such as those containing the heavy mesons, pentaquarks and so on [37–44]. Apart from the charm system, the bottom to charmed baryon nonleptonic decays have been recently analyzed in the LF formalism [45]. For a review on the comprehensive introduction of the LF QCD and its vacuum structure, one can refer to Ref. [35]. For the LF constituent quark

model (LFCQM), we recommend Ref. [36] and references therein. The advantage of LFCQM is that we can boost the reference frame without changing the equation of motion because of the commutativity of the LF Hamiltonian and boost generators. It provides us with a great convenience to calculate the wave-function in different inertial frames because of the recoil effects in the transition form factors.

This paper is organized as follows. We first present our formal calculations of the branching ratios and averaged decay asymmetries in terms of the helicity amplitudes, the baryonic states in LFCQM, and the baryonic transition form factors in Sec. II. In Sec. III, we show our numerical results and compare them with those in the literature. In Sec. IV, we give our conclusions.

II. FORMALISM

A. Helicity Amplitudes and Observables

The effective Hamiltonian for the anti-triplet charmed baryon semi-leptonic weak decays can be written as

$$\mathcal{H}_{eff} = \frac{G_F}{\sqrt{2}} V_{cq} (\bar{\nu}_\ell \ell)_{V-A} (\bar{q} c)_{V-A} \quad (1)$$

where G_F is the Fermi constant, V_{cq} is the CKM matrix element, and $(\bar{\ell}\nu_\ell)_{V-A}$ and $(\bar{q}c)_{V-A}$ denote as the usual $V-A$ currents $\bar{\ell}\gamma^\mu(1-\gamma_5)\nu_\ell$ and $\bar{q}\gamma_\mu(1-\gamma_5)c$ with $q = d, s$, respectively. The weak transition amplitudes of the anti-triplet charmed baryons are given by

$$\mathcal{A}(\mathbf{B}_c \rightarrow \mathbf{B}_n \ell^+ \nu_\ell) = \frac{G_F}{\sqrt{2}} V_{cq} \bar{\ell}\gamma^\mu(1-\gamma_5)\nu_\ell \langle \mathbf{B}_n | \bar{q}\gamma_\mu(1-\gamma_5)c | \mathbf{B}_c \rangle \quad (2)$$

where the baryon transition matrix elements are parameterized by

$$\begin{aligned} & \langle \mathbf{B}_n, p_f, S'_z | \bar{q}\gamma_\mu(1-\gamma_5)c | \mathbf{B}_c, p_i, S_z \rangle \\ &= \bar{u}_{\mathbf{B}_n}(p_f, S'_z) \left[\gamma_\mu f_1(k^2) - i\sigma_{\mu\nu} \frac{k^\nu}{M_{\mathbf{B}_c}} f_2(k^2) + f_3(k^2) \frac{k_\mu}{M_{\mathbf{B}_c}} \right] u_{\mathbf{B}_c}(p_i, S_z) \\ & - \bar{u}_{\mathbf{B}_n}(p_f, S'_z) \left[\gamma_\mu g_1(k^2) - i\sigma_{\mu\nu} \frac{k^\nu}{M_{\mathbf{B}_c}} g_2(k^2) + g_3(k^2) \frac{k_\mu}{M_{\mathbf{B}_c}} \right] \gamma_5 u_{\mathbf{B}_c}(p_i, S_z) \end{aligned} \quad (3)$$

with $k^\mu = p_i^\mu - p_f^\mu$, $\sigma_{\mu\nu} = \frac{i}{2} [\gamma_\mu, \gamma_\nu]$, and $f_i(k^2)$ and $g_i(k^2)$ being the form factors describing the non-perturbative QCD effect in the time-like range of $m_\ell^2 < k^2 < (M_{\mathbf{B}_c} - M_{\mathbf{B}_n})^2$. We introduce a set of helicity amplitudes $H_{\lambda_2 \lambda_W}^{V(A)}$ to calculate the decay branching ratios

and other physical quantities, where λ_2 and λ_W represent the helicity quantum numbers of the daughter baryon and off-shell W^+ boson in the decay processes, respectively. These amplitudes give more intuitive physical pictures about the helicity structures of the decay processes. Furthermore, when we evaluate the asymmetries of these processes, such as the integrated (averaged) decay asymmetry, also known as the longitudinal polarization of the daughter baryon, these amplitudes result in much simpler expressions than the traditional ones. Relations between the helicity amplitudes and form factors are given by[33, 46]

$$\begin{aligned}
H_{\frac{1}{2}1}^V &= \sqrt{2K_-} \left(-f_1(k^2) - \frac{M_{\mathbf{B}_c} + M_{\mathbf{B}_n}}{M_{\mathbf{B}_c}} f_2(k^2) \right), \\
H_{\frac{1}{2}0}^V &= \frac{\sqrt{K_-}}{\sqrt{k^2}} \left((M_{\mathbf{B}_c} + M_{\mathbf{B}_n}) f_1(k^2) + \frac{k^2}{M_{\mathbf{B}_c}} f_2(k^2) \right), \\
H_{\frac{1}{2}t}^V &= \frac{\sqrt{K_+}}{\sqrt{k^2}} \left((M_{\mathbf{B}_c} + M_{\mathbf{B}_n}) f_1(k^2) + \frac{k^2}{M_{\mathbf{B}_c}} f_3(k^2) \right), \\
H_{\frac{1}{2}1}^A &= \sqrt{2K_+} \left(-g_1(k^2) - \frac{M_{\mathbf{B}_c} + M_{\mathbf{B}_n}}{M_{\mathbf{B}_c}} g_2(k^2) \right), \\
H_{\frac{1}{2}0}^A &= \frac{\sqrt{K_+}}{\sqrt{k^2}} \left((M_{\mathbf{B}_c} - M_{\mathbf{B}_n}) g_1(k^2) - \frac{k^2}{M_{\mathbf{B}_c}} g_2(k^2) \right), \\
H_{\frac{1}{2}t}^A &= \frac{\sqrt{K_-}}{\sqrt{k^2}} \left((M_{\mathbf{B}_c} - M_{\mathbf{B}_n}) g_1(k^2) - \frac{k^2}{M_{\mathbf{B}_c}} g_3(k^2) \right), \tag{4}
\end{aligned}$$

where $K_{\pm} = (M_{\mathbf{B}_c} \pm M_{\mathbf{B}_n})^2 - k^2$.

The differential decay widths and asymmetries can be expressed in the following analytic forms in terms of the helicity amplitudes with the non-vanishing lepton masses of m_ℓ [19],

$$\begin{aligned}
\frac{d\Gamma}{dk^2} &= \frac{1}{3} \frac{G_F^2}{(2\pi)^3} |V_{qc}|^2 \frac{(k^2 - m_\ell^2)^2 p}{8M_{\mathbf{B}_c}^2 k^2} \left[\left(1 + \frac{m_\ell^2}{2k^2} \right) \right. \\
&\quad \left. \left(\left| H_{\frac{1}{2}1} \right|^2 + \left| H_{-\frac{1}{2}-1} \right|^2 + \left| H_{\frac{1}{2}0} \right|^2 + \left| H_{-\frac{1}{2}0} \right|^2 \right) + \frac{3m_\ell^2}{2k^2} \left(\left| H_{\frac{1}{2}t} \right|^2 + \left| H_{-\frac{1}{2}t} \right|^2 \right) \right], \tag{5}
\end{aligned}$$

$$\langle \alpha(k^2) \rangle = \frac{\int dk^2 \frac{(k^2 - m_\ell^2)^2 p}{8M_{\mathbf{B}_c}^2 k^2} \left[\left(1 + \frac{m_\ell^2}{2k^2} \right) \left(\left| H_{\frac{1}{2}1} \right|^2 - \left| H_{-\frac{1}{2}-1} \right|^2 + \left| H_{\frac{1}{2}0} \right|^2 - \left| H_{-\frac{1}{2}0} \right|^2 \right) + \frac{3m_\ell^2}{2k^2} \left(\left| H_{\frac{1}{2}t} \right|^2 - \left| H_{-\frac{1}{2}t} \right|^2 \right) \right]}{\int dk^2 \frac{(k^2 - m_\ell^2)^2 p}{8M_{\mathbf{B}_c}^2 k^2} \left[\left(1 + \frac{m_\ell^2}{2k^2} \right) \left(\left| H_{\frac{1}{2}1} \right|^2 + \left| H_{-\frac{1}{2}-1} \right|^2 + \left| H_{\frac{1}{2}0} \right|^2 + \left| H_{-\frac{1}{2}0} \right|^2 \right) + \frac{3m_\ell^2}{2k^2} \left(\left| H_{\frac{1}{2}t} \right|^2 + \left| H_{-\frac{1}{2}t} \right|^2 \right) \right]}, \tag{6}$$

where $p = \sqrt{K_+ K_-} / 2M_{\mathbf{B}_c}$ and $H_{\lambda_2 \lambda_W} = H_{\lambda_2 \lambda_W}^V - H_{\lambda_2 \lambda_W}^A$.

B. Light Front Constituent Quark Model

From Eqs. (5) and (6), we see that as long as the time-like form factors are known, both branching ratios and averaged decay asymmetries can be determined. To calculate these

time-like form factors, we use LFCQM, in which a baryon is treated as a bound state of three constituent quarks quantized in the LF formalism and its state is denoted by the momentum P , canonical spin S and the z-direction projection of spin S_z , respectively. As a result, the baryon state can be expressed by [35, 36, 39, 47–49]

$$|\mathbf{B}, P, S, S_z\rangle = \int \{d^3\tilde{p}\} 2(2\pi)^3 \frac{1}{\sqrt{P^+}} \delta^3(\tilde{P} - \tilde{p}_1 - \tilde{p}_2 - \tilde{p}_3) \\ \times \sum_{\lambda_1, \lambda_2, \lambda_3} \Psi^{SS_z}(\tilde{p}_1, \tilde{p}_2, \tilde{p}_3, \lambda_1, \lambda_2, \lambda_3) C^{\alpha\beta\gamma} F_{abc} |q_\alpha^a(\tilde{p}_1, \lambda_1) q_\beta^b(\tilde{p}_2, \lambda_2) q_\gamma^c(\tilde{p}_3, \lambda_3)\rangle, \quad (7)$$

where $\Psi^{SS_z}(\tilde{p}_1, \tilde{p}_2, \tilde{p}_3, \lambda_1, \lambda_2, \lambda_3)$ is the vertex function describing the overlapping between the baryon and its constituents, which can be formally solved from the three-body Bethe-Salpeter equations, $C^{\alpha\beta\gamma}$ (F_{abc}) are the color (flavor) factors, λ_i and \tilde{p}_i with $i = 1, 2, 3$ are the LF helicities and 3-momenta of the on-mass-shell constituent quarks, defined as

$$\tilde{p}_i = (p_i^+, p_{i\perp}), \quad p_{i\perp} = (p_i^1, p_i^2), \quad p_i^- = \frac{m_i^2 + p_{i\perp}^2}{p_i^+}, \quad (8)$$

and $|q_\alpha^a(\tilde{p}, \lambda)\rangle$ and $\{d^3\tilde{p}\}$ correspond to the light front constituent quark states and the integral measure, given by

$$|q_\alpha^a(\tilde{p}, \lambda)\rangle = d_\alpha^{\dagger a}(\tilde{p}, \lambda)|0\rangle, \quad \{d^3\tilde{p}\} \equiv \prod_{i=1,2,3} \frac{dp_i^+ d^2 p_{i\perp}}{2(2\pi)^3}, \quad (9)$$

respectively, with the quark field operators satisfied the following anti-commutation relations

$$\{d_{\alpha'}^a(\tilde{p}', \lambda'), d_\alpha^{\dagger a}(\tilde{p}, \lambda)\} = 2(2\pi)^3 \delta^3(\tilde{p}' - \tilde{p}) \delta_{\lambda'\lambda} \delta_{\alpha'\alpha} \delta^{a'a}, \quad \delta^3(\tilde{p}) = \delta(p^+) \delta^2(p_\perp). \quad (10)$$

To separate the internal motion of the constituents from the bulk motion, we use the kinematic variables of (q_\perp, ξ) , (Q_\perp, η) and P_{tot} , given by

$$P_{tot} = \tilde{P}_1 + \tilde{P}_2 + \tilde{P}_3, \quad \xi = \frac{p_1^+}{p_1^+ + p_2^+}, \quad \eta = \frac{p_1^+ + p_2^+}{P_{tot}^+}, \\ q_\perp = (1 - \xi)p_{1\perp} - \xi p_{2\perp}, \quad Q_\perp = (1 - \eta)(p_{1\perp} + p_{2\perp}) - \eta p_{3\perp}, \quad (11)$$

where (q_\perp, ξ) and (Q_\perp, η) capture the relative motions between the first and second quarks, and the third and other two quarks, respectively. We consider the three constituent quarks in the baryon independently with suitable spin-flavor structures satisfying the Fermi statistics to have a correct baryon bound state system. The vertex function of $\Psi^{SS_z}(\tilde{p}_1, \tilde{p}_2, \tilde{p}_3, \lambda_1, \lambda_2, \lambda_3)$ in Eq. (7) can be further written into two parts [35, 36, 50],

$$\Psi^{SS_z}(\tilde{p}_1, \tilde{p}_2, \tilde{p}_3, \lambda_1, \lambda_2, \lambda_3) = \phi(q_\perp, \xi, Q_\perp, \eta) \Xi^{SS_z}(\lambda_1, \lambda_2, \lambda_3), \quad (12)$$

where $\phi(q_\perp, \xi, Q_\perp, \eta)$ is the momentum distribution of constituent quarks and $\Xi^{SS_z}(\lambda_1, \lambda_2, \lambda_3)$ represents the momentum-dependent spin wave function, given by

$$\Xi^{SS_z}(\lambda_1, \lambda_2, \lambda_3) = \sum_{s_1, s_2, s_3} \langle \lambda_1 | R_1^\dagger | s_1 \rangle \langle \lambda_2 | R_2^\dagger | s_2 \rangle \langle \lambda_3 | R_3^\dagger | s_3 \rangle \left\langle \frac{1}{2} s_1, \frac{1}{2} s_2, \frac{1}{2} s_3 \left| SS_z \right. \right\rangle, \quad (13)$$

with the $SU(2)$ Clebsch-Gordan coefficients of $\langle \frac{1}{2} s_1, \frac{1}{2} s_2, \frac{1}{2} s_3 | SS_z \rangle$, and R_i is the Melosh transformation matrix [36, 51], which corresponds to the i th constituent quark, expressed by

$$\begin{aligned} R_M(x, p_\perp, m, M) &= \frac{m + xM - i\vec{\sigma} \cdot (\vec{n} \times \vec{q})}{\sqrt{(m + xM)^2 + q_\perp^2}}, \\ R_1 &= R_M(\eta, Q_\perp, M_3, M) R_M(\xi, q_\perp, m_1, M_3), \\ R_2 &= R_M(\eta, Q_\perp, M_3, M) R_M(1 - \xi, -q_\perp, m_2, M_3), \\ R_3 &= R_M(1 - \eta, -Q_\perp, m_3, M). \end{aligned} \quad (14)$$

Here, $\vec{\sigma}$ stands for the Pauli matrix, $\vec{n} = (0, 0, 1)$, and M and M_3 are invariant masses of (q_\perp, ξ) and (Q_\perp, η) systems, represented by [36]

$$\begin{aligned} M_3^2 &= \frac{q_\perp^2}{\xi(1 - \xi)} + \frac{m_1^2}{\xi} + \frac{m_2^2}{1 - \xi}, \\ M^2 &= \frac{Q_\perp^2}{\eta(1 - \eta)} + \frac{M_3^2}{\eta} + \frac{m_3^2}{1 - \eta}, \end{aligned} \quad (15)$$

respectively.

The spin-flavor structures of \mathbf{B}_c and \mathbf{B}_n are given by

$$\begin{aligned} |\mathbf{B}_c\rangle &= \frac{1}{\sqrt{6}} [\phi_3 \chi^{\rho^3} (|q_1 q_2 c\rangle - |q_2 q_1 c\rangle) + \phi_2 \chi^{\rho^2} (|q_1 c q_2\rangle - |q_2 c q_1\rangle) + \phi_1 \chi^{\rho^1} (|c q_1 q_2\rangle - |c q_2 q_1\rangle)], \\ |\Lambda^0\rangle &= \frac{1}{\sqrt{6}} \phi [\chi^{\rho^3} (|dus\rangle - |uds\rangle) + \chi^{\rho^2} (|dsu\rangle - |usd\rangle) + \chi^{\rho^1} (|sdu\rangle - |sud\rangle)], \\ |\Sigma^0\rangle &= \frac{1}{\sqrt{6}} \phi [\chi^{\lambda^3} (|dus\rangle + |uds\rangle) + \chi^{\lambda^2} (|dsu\rangle + |usd\rangle) + \chi^{\lambda^1} (|sdu\rangle + |sud\rangle)], \\ |B_n\rangle &= \frac{1}{\sqrt{3}} \phi [\chi^{\lambda^3} |q_1 q_1 q_2\rangle + \chi^{\lambda^2} |q_1 q_2 q_1\rangle + \chi^{\lambda^1} |q_2 q_1 q_1\rangle], \end{aligned} \quad (16)$$

where $q_{1(2)} = u, d, s$, $B_n = (N, \Xi, \Sigma^+, \Sigma^-)$, $\phi_{(i)}$ is the momentum distribution of the constituents with the corresponding spin-flavor configuration, and

$$\chi_\uparrow^{\rho^3} = \frac{1}{\sqrt{2}} (|\uparrow\downarrow\uparrow\rangle - |\downarrow\uparrow\uparrow\rangle), \quad \chi_\uparrow^{\lambda^3} = \frac{1}{\sqrt{6}} (|\uparrow\downarrow\uparrow\rangle + |\downarrow\uparrow\uparrow\rangle - 2|\uparrow\uparrow\downarrow\rangle), \quad (17)$$

In principle, one could solve $\phi_{(i)}$ from the Bethe-Salpeter equation with an explicit QCD-inspired potential but it is beyond the scope of this paper. Nonetheless, we use a Gaussian

type distribution with the phenomenological shape parameters β_Q and β_q to describe the relative motions of constituents. Consequently, we represent the LF kinematic variables (ξ, q_\perp) and (η, Q_\perp) in the forms of ordinary 3-momenta $\mathbf{q} = (q_\perp, q_z)$ and $\mathbf{Q} = (Q_\perp, Q_z)$:

$$\begin{aligned}\phi &= \mathcal{N} \sqrt{\frac{\partial q_z}{\partial \xi} \frac{\partial Q_z}{\partial \eta}} e^{-\frac{\mathbf{Q}^2}{2\beta_Q^2} - \frac{\mathbf{q}^2}{2\beta_q^2}}, \\ q_z &= \frac{\xi M_3}{2} - \frac{m_1^2 + q_\perp^2}{2M_3\xi}, \quad Q_z = \frac{\eta M}{2} - \frac{M_3^2 + Q_\perp^2}{2M\eta},\end{aligned}\quad (18)$$

where \mathcal{N} is the normalization constant. Since the one-particle baryonic state is normalized as

$$\langle \mathbf{B}, P', S', S'_z | \mathbf{B}, P, S, S_z \rangle = 2(2\pi)^3 P^+ \delta^3(\tilde{P}' - \tilde{P}) \delta_{S'_z S_z}, \quad (19)$$

the normalization condition of the momentum wave function is given by

$$\frac{1}{2^2(2\pi)^6} \int d\xi d\eta d^2 q_\perp d^2 Q_\perp |\phi_{(3)}|^2 = 1. \quad (20)$$

In this paper, we take different shape parameters of β_q and β_Q in the momentum wave functions ϕ_i to describe the scalar diquark effects in \mathbf{B}_c . On the other hand, we assume the momentum-distribution function ϕ of octet baryons \mathbf{B}_n is flavor symmetric for all constituents. In other words, the $SU(3)_f$ flavor symmetry is hold in the momentum wave function of \mathbf{B}_n . As a result, the shape parameters of ϕ are equal, *i.e.* $\beta_{Q\mathbf{B}_n} = \beta_{q\mathbf{B}_n} = \beta_{\mathbf{B}_n}$. Note that there is no $SU(6)$ spin-flavor symmetry in \mathbf{B}_c and \mathbf{B}_n because of the momentum-dependent Melosh transformation even though the forms of these states are similar to those with the $SU(6)$ spin-flavor wave functions.

C. Transition form factors

We pick the $\bar{q}\gamma^+(1 - \gamma_5)c$ current or so-called “good component” of the baryon transition amplitudes

$$\begin{aligned}& \langle \mathbf{B}_n, p_f, S'_z | \bar{q}\gamma^+(1 - \gamma_5)c | \mathbf{B}_c, p_i, S_z \rangle \\ &= \bar{u}_{\mathbf{B}_n}(p_f, S'_z) \left[\gamma^+ f_1(k^2) - i\sigma^{+\nu} \frac{k_\nu}{M_{\mathbf{B}_c}} f_2(k^2) + f_3(k^2) \frac{k^+}{M_{\mathbf{B}_c}} \right] u_{\mathbf{B}_c}(p_i, S_z) \\ &- \bar{u}_{\mathbf{B}_n}(p_f, S'_z) \left[\gamma^+ g_1(k^2) - i\sigma^{+\nu} \frac{k_\nu}{M_{\mathbf{B}_c}} g_2(k^2) + g_3(k^2) \frac{k^+}{M_{\mathbf{B}_c}} \right] \gamma_5 u_{\mathbf{B}_c}(p_i, S_z)\end{aligned}\quad (21)$$

and choose the frame such that $p_{i(f)}^+$ is conserved ($k^+ = 0, k^2 = -k_\perp^2$) to calculate the form factors to avoid zero-mode contributions and other x^+ -ordered diagrams in the LF formalism [35, 36]. The Matrix elements of the vector and axial-vector currents at quark level correspond to three different lowest-order Feynman diagrams as shown in Fig. 1. Since the spin-flavor-momentum wave functions of baryons are totally symmetric under the permutation of constituents, we have that $(a) + (b) + (c) = 3(a) = 3(b) = 3(c)$ [36]. We only present the calculation for the diagram (c), which contains simpler and cleaner forms with our notation $(q_\perp, Q_\perp, \xi, \eta)$ as a demonstration. We can extract the form factors from the matrix elements through the relations

$$\begin{aligned}
f_1(k^2) &= \frac{1}{2p_i^+} \langle \mathbf{B}_n, p_f, \uparrow | \bar{q} \gamma^+ c | \mathbf{B}_c, p_i, \uparrow \rangle, \\
f_2(k^2) &= \frac{1}{2p_i^+} \frac{M_{\mathbf{B}_c}}{k_\perp} \langle \mathbf{B}_n, p_f, \uparrow | \bar{q} \gamma^+ c | \mathbf{B}_c, p_i, \downarrow \rangle, \\
g_1(k^2) &= \frac{1}{2p_i^+} \langle \mathbf{B}_n, p_f, \uparrow | \bar{q} \gamma^+ \gamma_5 c | \mathbf{B}_c, p_i, \uparrow \rangle, \\
g_2(k^2) &= \frac{1}{2p_i^+} \frac{M_{\mathbf{B}_c}}{k_\perp} \langle \mathbf{B}_n, p_f, \uparrow | \bar{q} \gamma^+ \gamma_5 | \mathbf{B}_c, p_i, \downarrow \rangle.
\end{aligned} \tag{22}$$

Note that f_3 and g_3 are not available when $k^+ = 0$, but they are negligible because of the suppressions of $k^2/M_{\mathbf{B}_c}^2$. In fact, f_3 and g_3 are only associated with $H_{\frac{1}{2}t}^{V(A)}$ which do not contribute to the semileptonic decays in the massless lepton limit [19]. As a result, we can safely set both f_3 and g_3 to be 0 in this study. With the help of the momentum distribution functions and Melosh transformation matrix in Eq. (7), the transition matrix elements can

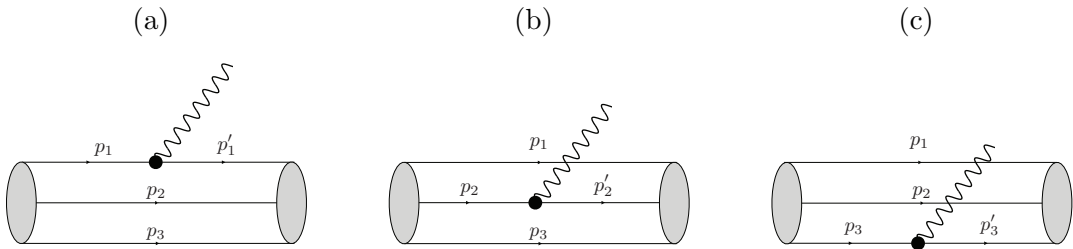


FIG. 1. Feynman diagrams for the baryonic weak transitions at the lowest order, where the sign of “•” denotes the V-A current vertex, where (a) $p_1' - p_1 = k$, (b) $p_2' - p_2 = k$ and (c) $p_3' - p_3 = k$.

be written as

$$\begin{aligned}
& \langle \mathbf{B}_n, p_f, S'_z | \bar{q} \gamma^+ (\gamma^5) c | \mathbf{B}_c, p_i, S_z \rangle \\
&= \frac{1}{2^2 (2\pi)^6} \int d\xi d\eta d^2 q_\perp d^2 Q_\perp \phi(q'_\perp, \xi, Q'_\perp, \eta) \phi_3(q_\perp, \xi, Q_\perp, \eta) F^{lmn} F_{ijk} \delta_l^i \delta_m^j \\
&\times \sum_{s_1, s_2, s_3} \sum_{s'_1, s'_2, s'_3} \langle S', S'_z | s'_1, s'_2, s'_3 \rangle \langle s_1, s_2, s_3 | S, S_z \rangle \langle s'_1 | R'_1 R_1^\dagger | s_1 \rangle \langle s'_2 | R'_2 R_2^\dagger | s_2 \rangle \\
&\times 2P^+ (3\delta_n^q \delta_c^k) \langle s'_3 | R'_3 \sum_{\lambda'_3 \lambda_3} \left(\delta_{\lambda'_3}^{\lambda_3} ([\sigma_z]_{\lambda'_3}^{\lambda_3}) | \lambda'_3 \rangle \langle \lambda_3 | \right) R_3^\dagger | s_3 \rangle, \tag{23}
\end{aligned}$$

where the indices of q and c in the delta symbols correspond to the quark flavors in the $\bar{q} \gamma^+ (\gamma^5) c$ current, $q'_\perp = q_\perp$ and $Q'_\perp = Q_\perp + k_\perp$. Using Eqs. (22) and (23), we find that

$$\begin{aligned}
f_1(k^2) &= \frac{3}{2^2 (2\pi)^6} \int d\xi d\eta d^2 q_\perp d^2 Q_\perp \phi(q'_\perp, \xi, Q'_\perp, \eta) \phi_3(q_\perp, \xi, Q_\perp, \eta) (F^{lmn} F_{ijk} \delta_n^q \delta_c^k \delta_l^i \delta_m^j) \\
&\times \sum_{s_1, s_2, s_3} \sum_{s'_1, s'_2, s'_3} \langle S', \uparrow | s'_1, s'_2, s'_3 \rangle \langle s_1, s_2, s_3 | S, \uparrow \rangle \prod_{i=1,2,3} \langle s'_i | R'_i R_i^\dagger | s_i \rangle, \tag{24}
\end{aligned}$$

$$\begin{aligned}
g_1(k^2) &= \frac{3}{2^2 (2\pi)^6} \int d\xi d\eta d^2 q_\perp d^2 Q_\perp \phi(q'_\perp, \xi, Q'_\perp, \eta) \phi_3(q_\perp, \xi, Q_\perp, \eta) (F^{lmn} F_{ijk} \delta_n^q \delta_c^k \delta_l^i \delta_m^j) \\
&\times \sum_{s_1, s_2, s_3} \sum_{s'_1, s'_2, s'_3} \langle S', \uparrow | s'_1, s'_2, s'_3 \rangle \langle s_1, s_2, s_3 | S, \uparrow \rangle \prod_{i=1,2} \langle s'_i | R'_i R_i^\dagger | s_i \rangle \langle s'_3 | R'_3 \sigma_z R_3^\dagger | s_3 \rangle, \tag{25}
\end{aligned}$$

$$\begin{aligned}
f_2(k^2) &= \frac{3}{2^2 (2\pi)^6} \frac{M_{\mathbf{B}_c}}{k_\perp} \int d\xi d\eta d^2 q_\perp d^2 Q_\perp \phi(q'_\perp, \xi, Q'_\perp, \eta) \phi_3(q_\perp, \xi, Q_\perp, \eta) (F^{lmn} F_{ijk} \delta_n^q \delta_c^k \delta_l^i \delta_m^j) \\
&\times \sum_{s_1, s_2, s_3} \sum_{s'_1, s'_2, s'_3} \langle S', \uparrow | s'_1, s'_2, s'_3 \rangle \langle s_1, s_2, s_3 | S, \downarrow \rangle \prod_{i=1,2,3} \langle s'_i | R'_i R_i^\dagger | s_i \rangle, \tag{26}
\end{aligned}$$

$$\begin{aligned}
g_2(k^2) &= \frac{3}{2^2 (2\pi)^6} \frac{M_{\mathbf{B}_c}}{k_\perp} \int d\xi d\eta d^2 q_\perp d^2 Q_\perp \phi(q'_\perp, \xi, Q'_\perp, \eta) \phi_3(q_\perp, \xi, Q_\perp, \eta) (F^{lmn} F_{ijk} \delta_n^q \delta_c^k \delta_l^i \delta_m^j) \\
&\times \sum_{s_1, s_2, s_3} \sum_{s'_1, s'_2, s'_3} \langle S', \uparrow | s'_1, s'_2, s'_3 \rangle \langle s_1, s_2, s_3 | S, \downarrow \rangle \prod_{i=1,2} \langle s'_i | R'_i R_i^\dagger | s_i \rangle \langle s'_3 | R'_3 \sigma_z R_3^\dagger | s_3 \rangle. \tag{27}
\end{aligned}$$

III. NUMERICAL RESULTS

To find out the decay branching ratios and averaged asymmetries in the helicity formalism, we first calculate the transition form factors with LFCQM. By imposing the condition $k^+ = 0$, the form factors can be evaluated only in the space-like region ($k^2 = -k_\perp^2$) instead of the time-like one. Nonetheless, we still can extract the time-like information of the form factors via analytically continuations [39, 48, 52, 53].

TABLE I. Values of the constituent quark masses (m_i) and shape parameters ($\beta_{q\mathbf{B}_c}$, $\beta_{Q\mathbf{B}_c}$, $\beta_{\mathbf{B}_n}$) in units of GeV.

m_c	m_s	m_d	m_c	$\beta_{q\Lambda_c}$	$\beta_{Q\Lambda_c}$
1.3	0.4	0.26	0.26	0.44	0.53
$\beta_{q\Xi_c}$	$\beta_{Q\Xi_c}$	β_N	β_Λ	β_Σ	β_Ξ
0.49	0.53	0.32	0.34	0.34	0.37

We fit $f_{1(2)}(k^2)$ and $g_{1(2)}(k^2)$ with the analytic functions in the space-like region with the following form

$$F(k^2) = \frac{F(0)}{1 - q_1 k^2 + q_2 k^4}. \quad (28)$$

We employ the numerical values of the constituent quark masses and shape parameters in Table. I. The values of the shape parameters can be determined approximately by the calculations in the mesonic cases [47, 54]. Because the strength of the quark-quark pairs is a half of the quark-anti-quark one [47], we will get the shape parameters of the quark pairs, which are approximately $\sqrt{2}$ smaller than those in the mesonic cases.

We adopt $\beta_{q\Lambda_c} \simeq 2(\beta_{u\bar{d}}/\sqrt{2})$ and $\beta_{q\Xi_c} \simeq 2(\beta_{s\bar{u}(\bar{d})}/\sqrt{2})$, where the factor of 2 comes from the effects of the diquark clustering, making the light quark pairs to be more compact in \mathbf{B}_c baryons. For the octet baryons of \mathbf{B}_n , we assume that the $SU(3)_f$ flavor symmetry is hold, and therefore, the shape parameters is flavor symmetric for each constituent, *i.e.* $\beta_Q = \beta_q$. As a result, we approximate the shape parameters of the octet baryons equal to the mesonic ones by effectively treating any pair of two constituents as a heavier anti-quark. By using Eqs. (24)-(27), we numerically compute 32 points for all form factors from $k^2 = 0$ to $k^2 = -9.7 \text{ GeV}^2$ and fit them with the MATLAB curve fitting toolbox. We present our fitting results of the form factors in Tables II, III and IV, and our predictions of the branching ratios and asymmetry parameters in Table V. The comparisons with different theoretical models are presented in Tables VI, VII and VIII, respectively.

The uncertainties of our results mainly arise from the extrapolations by the analytical continuation method. The magnitudes of average asymmetry parameters predicted by LFCQM almost reach their extremums in all channels. As shown in Tables VI-VIII, we obtain that $\mathcal{B}(\Lambda_c^+ \rightarrow \Lambda e^+ \nu_e) = (3.55 \pm 1.04)\%$, $\mathcal{B}(\Xi_c^+ \rightarrow \Xi^0 e^+ \nu_e) = (11.3 \pm 3.4)\%$ and $\mathcal{B}(\Xi_c^0 \rightarrow \Xi^- e^+ \nu_e) = (3.49 \pm 0.95)\%$, which are all consistent with the current data from

TABLE II. Fitting results of the $\Lambda_c^+ \rightarrow \mathbf{B}_n$ form factors in LFCQM

$\Lambda_c^+ \rightarrow \Lambda$				
	f_1	f_2	g_1	g_2
$F(0)$	0.67 ± 0.01	0.76 ± 0.02	0.59 ± 0.01	$(3.8 \pm 1.2) \times 10^{-3}$
q_1	1.48 ± 0.31	1.44 ± 0.30	1.22 ± 0.28	4.99 ± 17.6
q_2	2.29 ± 0.49	2.23 ± 0.48	1.82 ± 0.39	24.8 ± 95.8
$\Lambda_c^+ \rightarrow n$				
	f_1	f_2	g_1	g_2
$F(0)$	0.83 ± 0.01	1.05 ± 0.02	0.71 ± 0.01	0.27 ± 0.01
q_1	1.25 ± 0.36	1.20 ± 0.30	0.94 ± 0.28	1.37 ± 0.40
q_2	1.85 ± 0.68	1.78 ± 0.48	1.36 ± 0.39	2.08 ± 0.83

 TABLE III. Fitting results of the $\Xi_c^+ \rightarrow \mathbf{B}_n$ form factors in LFCQM,

$\Xi_c^+ \rightarrow \Xi^0$				
	f_1	f_2	g_1	g_2
$F(0)$	0.77 ± 0.02	0.96 ± 0.02	0.69 ± 0.01	$(6.8 \pm 0.3) \times 10^{-3}$
q_1	1.50 ± 0.31	1.45 ± 0.31	1.25 ± 0.28	2.00 ± 0.76
q_2	2.30 ± 0.49	2.26 ± 0.49	1.85 ± 0.39	3.00 ± 1.41
$\Xi_c^+ \rightarrow \Sigma^0$				
	f_1	f_2	g_1	g_2
$F(0)$	0.52 ± 0.01	0.70 ± 0.02	0.45 ± 0.01	0.08 ± 0.01
q_1	1.49 ± 0.32	1.43 ± 0.33	1.18 ± 0.28	1.88 ± 0.39
q_2	2.35 ± 0.51	2.38 ± 0.53	1.79 ± 0.38	2.88 ± 0.67
$\Xi_c^+ \rightarrow \Lambda$				
	f_1	f_2	g_1	g_2
$F(0)$	0.28 ± 0.01	0.38 ± 0.01	0.25 ± 0.01	0.04 ± 0.01
q_1	1.50 ± 0.31	1.35 ± 0.51	1.18 ± 0.28	1.71 ± 0.38
q_2	2.32 ± 0.50	2.30 ± 0.81	1.77 ± 0.38	2.78 ± 0.66

TABLE IV. Fitting results of the $\Xi_c^0 \rightarrow \mathbf{B}_n$ form factors in LFCQM,

$\Xi_c^0 \rightarrow \Xi^-$				
	f_1	f_2	g_1	g_2
$F(0)$	0.74 ± 0.02	0.96 ± 0.02	0.69 ± 0.01	$(6.8 \pm 0.3) \times 10^{-3}$
q_1	1.50 ± 0.31	1.47 ± 0.31	1.21 ± 0.28	2.00 ± 0.76
q_2	2.30 ± 0.50	2.25 ± 0.48	1.98 ± 0.39	3.00 ± 1.41
$\Xi_c^0 \rightarrow \Sigma^-$				
	f_1	f_2	g_1	g_2
$F(0)$	0.73 ± 0.01	0.99 ± 0.02	0.63 ± 0.01	0.11 ± 0.01
q_1	1.49 ± 0.32	1.43 ± 0.33	1.18 ± 0.28	1.88 ± 0.39
q_2	2.35 ± 0.51	2.38 ± 0.53	1.79 ± 0.38	2.88 ± 0.70

TABLE V. Predictions of the decay branching ratios and asymmetry parameters

	$\ell^+ = e^+$		$\ell^+ = \mu^+$	
	$\mathcal{B}(\%)$	α	$\mathcal{B}(\%)$	α
$\Lambda_c^+ \rightarrow \Lambda \ell^+ \nu_\ell$	3.55 ± 1.04	-0.97 ± 0.03	3.40 ± 1.02	-0.98 ± 0.02
$\Lambda_c^+ \rightarrow n \ell^+ \nu_\ell$	0.36 ± 0.15	-0.96 ± 0.04	0.34 ± 0.15	-0.96 ± 0.04
$\Xi_c^+ \rightarrow \Xi^0 \ell^+ \nu_\ell$	11.3 ± 3.35	-0.97 ± 0.03	10.8 ± 3.3	-0.97 ± 0.03
$\Xi_c^+ \rightarrow \Sigma^0 \ell^+ \nu_\ell$	0.33 ± 0.09	-0.98 ± 0.01	0.31 ± 0.09	-0.98 ± 0.02
$\Xi_c^+ \rightarrow \Lambda \ell^+ \nu_\ell$	0.12 ± 0.04	-0.98 ± 0.02	0.11 ± 0.05	-0.98 ± 0.02
$\Xi_c^0 \rightarrow \Xi^- \ell^+ \nu_\ell$	3.49 ± 0.95	-0.98 ± 0.02	3.34 ± 0.94	-0.98 ± 0.02
$\Xi_c^0 \rightarrow \Sigma^- \ell^+ \nu_\ell$	0.22 ± 0.06	-0.98 ± 0.02	0.21 ± 0.06	-0.98 ± 0.02

PDG [4] and the BELLE experiments [1, 2]. Our branching ratios are also consistent with the predictions of the relativistic quark model (RQM) [28, 29], the covariant constituent quark model (CCQM) [30] and the $SU(3)_F$ approach [19]. The results given by the LF formalism [33] and heavy quark effective theory (HQET) [25] are half of ours because they choose the spin-flavor wave function of \mathbf{B}_c to be $c(q_1 q_2 - q_2 q_1) \chi_{s_z}^{\rho_3}$ instead of the totally symmetric one. The averaged asymmetry parameter predicted by LFCQM in $\Lambda_c^+ \rightarrow \Lambda e^+ \nu_e$ is 10% lower than the data. Since we do not consider any parameters about spin interactions

TABLE VI. Our results of $\Lambda_c^+ \rightarrow \mathbf{B}_n e^+ \nu_e$ decays in comparisons with the experimental data and those in various calculations in the literature.

	$\Lambda_c^+ \rightarrow \Lambda e^+ \nu_e$		$\Lambda_c^+ \rightarrow n e^+ \nu_e$	
	$\mathcal{B}(\%)$	α	$\mathcal{B}(\%)$	α
LFCQM	3.55 ± 1.04	-0.97 ± 0.03	0.36 ± 0.15	-0.96 ± 0.04
Data [4]	3.6 ± 0.4	-0.86 ± 0.04	-	-
$SU(3)$ [19]	3.2 ± 0.3	-0.86 ± 0.04	0.51 ± 0.04	-0.89 ± 0.04
RQM [28, 29]	3.25	-0.86	0.268	-0.91
HQET [25]	1.42	-	-	-
LF [33]	1.63	-	0.201	-
MBM (NRQM) [34]	2.6 (3.2)	-	0.20 (0.30)	-
LQCD [26, 27]	3.80 ± 0.22	-	0.41 ± 0.03	-
CCQM [30]	2.78	-0.87	0.20	-
LCSR [31, 32]	3.0 ± 0.3	-	8.69 ± 2.89	-

in our phenomenological wave functions, the helicity-structure-related results, such as the decay asymmetries, are clearly not precise enough to explain the experimental data. On the other hand, the prediction from RQM and the $SU(3)_f$ approach are almost the same as the data. Since the authors for RQM in Refs. [28, 29] have considered a comprehensive QCD-inspired potential including the chromomagnetic effect, their results are more close to the experimental values than ours. Meanwhile, the $SU(3)_f$ approach is a model independent way to analyze $\mathbf{B}_c \rightarrow \mathbf{B}_n \ell^+ \nu_\ell$ decays, which automatically includes the information related to the spin interaction when the asymmetry parameters are used as the fitting inputs. Clearly, our results of the asymmetry parameters could be improved by considering the full QCD potential and its solutions.

IV. CONCLUSIONS

We have systematically studied the semi-leptonic decays of $\mathbf{B}_c \rightarrow \mathbf{B}_n \ell^+ \nu_\ell$ in LFCQM. By requiring the constituents in the baryonic states to obey the Fermi statistics, we are able to determine the overall spin-flavor-momentum structures of the baryons. We assume that

TABLE VII. Our results of $\Xi_c^+ \rightarrow \mathbf{B}_n e^+ \nu_e$ decays in comparisons with the experimental data and those in various calculations in the literature.

	$\Xi_c^+ \rightarrow \Xi^0 e^+ \nu_e$		$\Xi_c^+ \rightarrow \Sigma^0 e^+ \nu_e$ $\Xi_c^+ \rightarrow \Lambda e^+ \nu_e$	
	$\mathcal{B}(\%)$	α	$\mathcal{B}(\%)$	α
LFCQM	11.3 ± 3.35	-0.97 ± 0.03	0.33 ± 0.09 0.12 ± 0.04	-0.98 ± 0.01 -0.98 ± 0.02
Data [2, 4]	$6.6^{+3.7}_{-3.5}$	-	- -	- -
$SU(3)$ [19]	10.7 ± 0.9	-0.83 ± 0.04	0.46 ± 0.04 0.22 ± 0.02	-0.85 ± 0.04 -0.86 ± 0.04
RQM [29]	9.40	-0.80	- 0.13	- -0.84
LF [33]	5.39	-	0.19 0.08	- -
MBM (NRQM) [34]	11.1 (13.3)	-	0.28 (0.41) 0.09 (0.14)	- -

TABLE VIII. Our results of $\Xi_c^0 \rightarrow \mathbf{B}_n e^+ \nu_e$ decays in comparisons with the experimental data and those in various calculations in the literature.

	$\Xi_c^0 \rightarrow \Xi^- e^+ \nu_e$		$\Xi_c^0 \rightarrow \Sigma^- e^+ \nu_e$	
	$\mathcal{B}(\%)$	α	$\mathcal{B}(\%)$	α
LFCQM	3.49 ± 0.95	-0.98 ± 0.03	0.22 ± 0.06	-0.98 ± 0.02
Data [1, 4]	1.8 ± 1.2	-	-	-
$SU(3)$ [19]	3.7 ± 0.3	-0.83 ± 0.04	0.33 ± 0.03	-0.85 ± 0.04
RQM [29]	2.38	-0.80	-	-
LF [33]	1.35	-	0.10	-
MBM (NRQM) [34]	3.55 (4.47)	-	0.19 (0.26)	-

the momentum distribution of \mathbf{B}_n is symmetric in flavor indices and any pair of two quarks can be effectively treated as a heavier anti-quark. We have found that $\mathcal{B}(\Lambda_c^+ \rightarrow \Lambda e^+ \nu_e) = (3.55 \pm 1.04)\%$, $\mathcal{B}(\Xi_c^+ \rightarrow \Xi^0 e^+ \nu_e) = (11.3 \pm 3.35)\%$ and $\mathcal{B}(\Xi_c^0 \rightarrow \Xi^- e^+ \nu_e) = (3.49 \pm 0.95)\%$ in LFCQM, which are consistent with the experimental data of $(3.6 \pm 0.4) \times 10^{-2}$ [4], $(6.6_{-3.5}^{+3.7}) \times 10^{-2}$ [2, 4] and $(1.8 \pm 1.2) \times 10^{-2}$ [1, 4] as well as the values predicted by $SU(3)_F$ [19], LQCD [26, 27], RQM [28], and CCQM [30], but twice larger than those in HQET [25] and LF [33]. We have also obtained that $\alpha(\Lambda_c^+ \rightarrow \Lambda e^+ \nu_e) = (-0.97 \pm 0.03)$ in LFCQM, which is 10% lower than the experimental data of -0.86 ± 0.04 [4]. The reason of this deviation may arise from the QCD spin-spin interacting effects, which are not included in our phenomenological wave functions. Our results of the averaged decay asymmetries could be improved if we consider the wave function solved from the full QCD potential. It is clear that our predicted values for the decay branching ratios and asymmetries in $\Xi_c^{+(0)} \rightarrow \mathbf{B}_n e^+ \nu_e$ could be tested in the ongoing experiments at LHCb and BELLEII.

ACKNOWLEDGMENTS

We would like to thank Prof. Chengping Shen for discussions. This work was supported in part by National Center for Theoretical Sciences and MoST (MoST-107-2119-M-007-013-MY3).

-
- [1] Y. B. Li *et al.* [Belle Collaboration], Phys. Rev. Lett. **122**, 082001 (2019).
 - [2] Y. B. Li *et al.* [Belle Collaboration], Phys. Rev. D **100**, 031101 (2019).
 - [3] R. Aaij *et al.* [LHCb Collaboration], Phys. Rev. D **100**, 032001 (2019).
 - [4] P. A. Zyla *et al.* [Particle Data Group], PTEP **2020**, 083C01 (2020).
 - [5] M. J. Savage and R. P. Springer, Phys. Rev. D **42**, 1527 (1990).
 - [6] M. J. Savage, Phys. Lett. B **257**, 414 (1991).
 - [7] C. D. Lu, W. Wang and F. S. Yu, Phys. Rev. D **93**, 056008 (2016).
 - [8] C. Q. Geng, Y. K. Hsiao, C. W. Liu and T. H. Tsai, JHEP **1711**, 147 (2017).
 - [9] W. Wang, Z. P. Xing and J. Xu, Eur. Phys. J. C **77**, 800 (2017).
 - [10] C. Q. Geng, Y. K. Hsiao, Y. H. Lin and L. L. Liu, Phys. Lett. B **776**, 265 (2018).

- [11] C. Q. Geng, Y. K. Hsiao, C. W. Liu and T. H. Tsai, Phys. Rev. D **97**, 073006 (2018); Eur. Phys. J. C **78**, 593 (2018).
- [12] D. Wang, P. F. Guo, W. H. Long and F. S. Yu, JHEP **1803**, 066 (2018).
- [13] X. G. He and W. Wang, Chin. Phys. C **42**, 103108 (2018).
- [14] C. Q. Geng, Y. K. Hsiao, C. W. Liu and T. H. Tsai, Phys. Rev. D **99**, 073003 (2019).
- [15] C. Q. Geng, C. W. Liu and T. H. Tsai, Phys. Lett. B **790**, 225 (2019); Phys. Lett. B **794**, 19 (2019).
- [16] C. Q. Geng, C. W. Liu, T. H. Tsai and Y. Yu, Phys. Rev. D **99**, 114022 (2019).
- [17] J. Y. Cen, C. Q. Geng, C. W. Liu and T. H. Tsai, Eur. Phys. J. C **79**, 946 (2019).
- [18] Y. K. Hsiao, Y. Yao and H. J. Zhao, Phys. Lett. B **792**, 35 (2019).
- [19] C. Q. Geng, C. W. Liu, T. H. Tsai and S. W. Yeh, Phys. Lett. B **792**, 214 (2019).
- [20] Y. Grossman and S. Schacht, JHEP **1907**, 020 (2019).
- [21] X. G. He, Y. J. Shi and W. Wang, Eur. Phys. J. C **80**, 359 (2020).
- [22] S. Roy, R. Sinha and N. G. Deshpande, Phys. Rev. D **101**, 036018 (2020).
- [23] C. Q. Geng, C. C. Lih, C. W. Liu and T. H. Tsai, Phys. Rev. D **101**, 094017 (2020).
- [24] C. P. Jia, D. Wang and F. S. Yu, Nucl. Phys. B **956**, 115048 (2020).
- [25] H. Y. Cheng and B. Tseng, Phys. Rev. D **53**, 1457 (1996).
- [26] S. Meinel, Phys. Rev. Lett. **118**, 082001 (2017).
- [27] S. Meinel, Phys. Rev. D **97**, 034511 (2018).
- [28] R. N. Faustov and V. O. Galkin, Eur. Phys. J. C **76**, 628 (2016).
- [29] R. N. Faustov and V. O. Galkin, Eur. Phys. J. C **79**, 695 (2019); Particles **3**, 208-222 (2020)
- [30] T. Gutsche, M. A. Ivanov, J. G. Korner, V. E. Lyubovitskij and P. Santorelli, Phys. Rev. D **93**, 034008 (2016).
- [31] Y. L. Liu, M. Q. Huang and D. W. Wang, Phys. Rev. D **80**, 074011 (2009)
- [32] K. Azizi, M. Bayar, Y. Sarac and H. Sundu, Phys. Rev. D **80**, 096007 (2009)
- [33] Z. X. Zhao, Chin. Phys. C **42**, 093101 (2018).
- [34] R. Perez-Marcial, R. Huerta, A. Garcia and M. Avila-Aoki, Phys. Rev. D **40**, 2955 (1989)
Erratum: [Phys. Rev. D **44**, 2203 (1991)].
- [35] W. M. Zhang, Chin. J. Phys. **32**, 717 (1994).
- [36] F. Schlumpf, hep-ph/9211255.
- [37] C. Q. Geng, C. C. Lih and W. M. Zhang, Phys. Rev. D **62**, 074017 (2000).

- [38] C. Q. Geng, C. W. Hwang and C. C. Liu, Phys. Rev. D **65**, 094037 (2002).
- [39] H. Y. Cheng, C. K. Chua and C. W. Hwang, Phys. Rev. D **70**, 034007 (2004).
- [40] C. Q. Geng, C. C. Lih and C. Xia, Eur. Phys. J. C **76**, 313 (2016).
- [41] H. Y. Cheng and X. W. Kang, Eur. Phys. J. C **77**, 587 (2017) Erratum: [Eur. Phys. J. C **77**, 863 (2017)].
- [42] Z. X. Zhao, Eur. Phys. J. C **78**, 756 (2018).
- [43] Z. P. Xing and Z. X. Zhao, Phys. Rev. D **98**, 056002 (2018).
- [44] Q. Chang, L. T. Wang and X. N. Li, JHEP **1912**, 102 (2019).
- [45] C. K. Chua, Phys. Rev. D **99**, 014023 (2019); Phys. Rev. D **100**, 034025 (2019).
- [46] A. Kadeer, J. G. Korner and U. Moosbrugger, Eur. Phys. J. C **59**, 27-47 (2009)
- [47] H. W. Ke, N. Hao and X. Q. Li, Eur. Phys. J. C **79**, 540 (2019).
- [48] H. W. Ke, X. Q. Li and Z. T. Wei, Phys. Rev. D **77**, 014020 (2008).
- [49] H. W. Ke, X. H. Yuan, X. Q. Li, Z. T. Wei and Y. X. Zhang, Phys. Rev. D **86**, 114005 (2012).
- [50] C. Lorce, B. Pasquini and M. Vanderhaeghen, JHEP **1105**, 041 (2011).
- [51] W. N. Polyzou, W. Glockle and H. Witala, Few Body Syst. **54**, 1667 (2013).
- [52] W. Jaus, Phys. Rev. D **44**, 2851 (1991).
- [53] W. Jaus, Phys. Rev. D **53**, 1349 (1996) Erratum: [Phys. Rev. D **54**, 5904 (1996)].
- [54] Q. Chang, X. N. Li, X. Q. Li, F. Su and Y. D. Yang, Phys. Rev. D **98**, 114018 (2018).